Progress In Electromagnetics Research C, Vol. 49, 89–96, 2014

Low Cost System for the Measurement of the Electromagnetic Microwave Emission by Hot Surfaces

Maurizio Tinti*

Abstract—Research centers and industries often need to measure the microwave electromagnetic emission of hot bodies, in order to calculate their temperature. It is well known that the most critical part of a microwave radiometer is its receiver, to obtain a very sensitive system that can also measure low emissions this needs, among other features, to be very sensitive, necessitating the use of expensive low noise amplifiers. For some time now, low-cost components for the reception of satellite TV have been available on the consumer market. These are known as Low Noise Block (LNB), and they include, as a front-end, an amplifier with very low intrinsic noise. In this study, we wanted to test the feasibility of designing and using a 12 GHz total power radiometer, using, as a front-end, an LNB. The system was tested, in different configurations, to measure the emission due to natural sources (Earth, Sun and a sunny wall).

1. INTRODUCTION

In this article, firstly we give a general description of radiometers and their problems. Then we describe our implementation, and finally we show some measurements performed with our system. Other works on this argument are described in [6–9].

Figure 1 shows the block diagram of a generic "total power" radiometer. The noise power coming from the body under observation is firstly amplified by a Radio Frequency (RF) amplifier. The next block is a mixer that converts the RF signal to the Intermediate Frequency (IF) signal, which is amplified by the IF amplifier and band limited by a band pass filter. The IF signal, like the RF signal, is comparable to a randomly modulated carrier wave. Its power is then measured by a square law detector. This is followed by a Low Frequency (LF) amplifier and by an integrator, whose time constant τ determines the minimum detectable temperature of the system [1]. This time constant is set so as to achieve a compromise between the conflicting demands of having a sufficiently short response time compared to the dynamics of the phenomena that the system observes and high receiver sensitivity.

Another factor which determines the minimum detectable temperature of the system is the noise figure of the front-end amplifier [1], which should be very low. In professional radiometers, expensive low-noise amplifiers are used to achieve this. In our project, we tested the possibility of using, as a front-end receiver, an LNB, which includes a very low noise amplifier.

The general problems of radiometers are extensively analyzed in [2, 3]. Their sensitivity is analyzed in [4].

A LNB is constituted by a corrugated truncated cone illuminator, two orthogonal dipoles (one for the reception of the horizontally polarized field and one for the reception of the vertically polarized field), a double very low noise HEMT front-end amplifier (for the two linear polarizations), an active mixer, a very stable local oscillator (OL) with a dielectric resonator (DRO), an interdigitated band filter, an Intermediate Frequency (IF) amplifier and a stabilizer of the working voltage. The outputs of

Received 9 February 2014, Accepted 11 April 2014, Scheduled 15 April 2014

* Corresponding author: Maurizio Tinti (maurizio.tinti@unibo.it).

The author is with the Department of Electrical, Electronic and Information, Engineering "Guglielmo Marconi", Università di Bologna, Bologna, Italy.

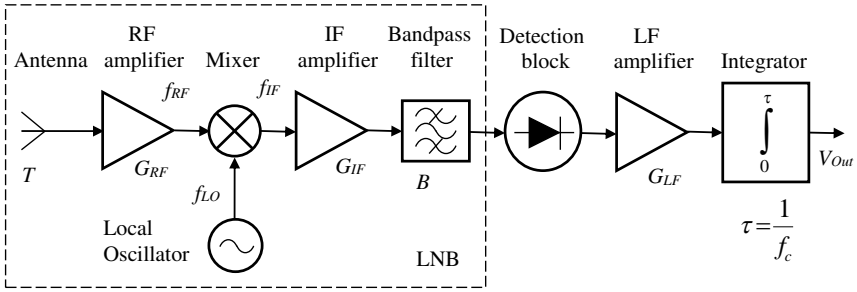

Figure 1. Block diagram of a "total power" radio telescope. We have indicated with: T the temperature of the antenna, G_{RF} the gain of the Radio Frequency (RF) amplifier, f_{RF} the frequency of the RF signal, f_{LO} the frequency of the local oscillator, f_{IF} the frequency of the Intermediate Frequency (IF) signal, G_{IF} the gain of the IF amplifier, B the bandwidth of the band pass filter, G_{LF} the gain of the Low Frequency (LF) amplifier, τ the time constant of the integrator.

the two amplifiers are connected to an adder and the selection of the polarization of the field that we want to receive is obtained inhibiting, with an appropriate voltage, the amplifier corresponding to the undesired polarization. This voltage is derived from the power supply, which can be, depending on the desired polarization, +12 V or +18 V and which is provided to the LNB through the antenna cable by the receiver that follows. The LNB amplifies the input signal (which is in a part of the Ku-band, the frequency range between 11 GHz and 12 GHz) and by means of the local oscillator converts it into the Intermediate Frequency (1–2 GHz). The total gain of the block is 60 dB and the bandwidth is about 1 GHz. Therefore the use of an LNB as a front-end receiver requires the insertion of a supply bridge between the LNB and the block that follows. The configuration of the measurement system appears to be that indicated by the block diagram of Figure 2.

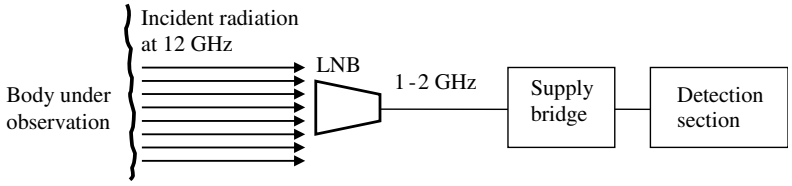

Figure 2. Block diagram of the measurement system.

2. RESOLUTION, SENSITIVITY AND MEASURING RANGE OF THE RADIOMETER

The LNB's truncated cone illuminator ends in a circular waveguide whose diameter is about 25 mm. Considering, in first approximation, the behavior of the illuminator as a circular aperture having diameter $d = 25$ mm, the LNB resolution, according to the Rayleigh criterion, is given by the first diffraction minimum of the aperture, which occurs for the angle [5]:

$$\alpha = 1.22\frac{\lambda}{d} \tag{1}$$

The frequency $\nu = 12$ GHz corresponds to the wavelength:

$$\lambda = \frac{c}{\nu} = \frac{3 \cdot 10^8}{12 \cdot 10^9} = 25\,\text{mm}$$

(it is indicated with c the speed of light in vacuum).

Substituting the numerical values of λ and d in (1), it is $\alpha = 1.22$ rad corresponding to about 60° (see Figure 3).

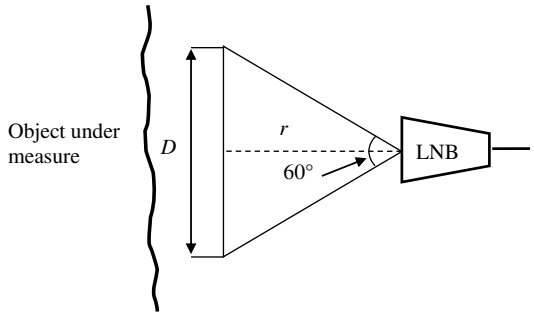

Figure 3. Calculation of the minimum dimensions of the object under measurement in respect of the distance of the object from the receiver.

The receiver works in the far field zone when its distance r from the body that it is measuring is greater than 3λ, or $r > 75\,\text{mm}$. This is the required minimum distance between the receiver and the body under test. The relationship between the diameter D of the circular surface subtended by the antenna beam and the distance r between the receiver and the body under measurement is:

$$D = \frac{2}{\sqrt{3}} r \tag{2}$$

The body under test, placed at a given distance r from the receiver, to occupy the entire surface subtended by the antenna beam, must have its smaller linear dimension greater than the dimension D calculated according to (2). The body under measurement must always have the smallest size greater than D calculated for r min, or 86.6 mm.

The equivalent noise temperature T_R of the radiometer is determined by that of the front-end amplifier. The front-end amplifier of the LNB that we used has, as indicated by the manufacturer, a noise figure $NF = 0.3\,\text{dB}$. Assuming the ambient temperature $T_0 = 290\,\text{K}$, it is [1]:

$$T_R = T_0 \left(10^{\frac{NF}{10}} - 1\right) = 20.7\,\text{K} \tag{3}$$

The noise power measured by the instrument is the sum of the noise power P_A received by the antenna and the noise power P_R generated inside the radiometer. In our case, since the object under measurement occupies the entire area subtended by the antenna beam, the Rayleigh-Jeans equation became [1]:

$$P_A = k \cdot T_A \cdot B \tag{4}$$

where: P_A is the noise power that the antenna receives from the object under measurement; $k = 1.38 \cdot 10^{-23}\,\text{J} \cdot \text{K}^{-1}$ is the Boltzmann constant; B is the bandwidth of the IF stage; T_A is the temperature of the object.

The noise power P_R generated inside the radiometer, corresponding to its equivalent noise temperature, T_R is:

$$P_R = k \cdot T_R \cdot B \tag{5}$$

To obtain the true value of the received noise power, we must subtract this noise power from the indication of the instrument.

The system temperature T_{sys}:

$$T_{sys} = T_A + T_R \tag{6}$$

depends on the antenna temperature T_A, that coincides with the temperature of the background that the antenna "sees" in absence of the body under measurement. Some examples are given in [7, 8]. In our measures we can assume as background the Cold Sky, that we consider at a temperature of $T_{Cold\ Sky} \approx 40\,\text{K}$ [9]. Therefore $T_{sys} \approx 60\,\text{K}$.

The minimum detectable temperature of the system $\Delta T_{\min}$ depends not only on the system temperature, but also on the bandwidth B of the receiver and on the time constant τ of the integrator that follows the detector [1]:

$$\Delta T_{\min} = \frac{T_{Sys}}{\sqrt{B \cdot \tau}} \tag{7}$$

In our system B and τ depend on the equipment that follows the LNB.

It should be observed that the secondary lobes of the radiation pattern of the LNB introduce a not accurately quantifiable source of noise that worsens the signal to noise ratio of the system ("signal" is the noise power emitted by the body under measurement; "noise" is the noise power emitted by all the surfaces that the antenna "sees" in addition to the body under measurement).

Substituting the bandwidth B of the filter and the detection range of the detecting block that follows the LNB in (5), it is possible to calculate the measuring range of the system.

3. IMPLEMENTATION OF THE SUPPLY BRIDGE FOR THE LNB

The supply bridge consists of a bias-tee that overlaps the voltage required to supply the LNB block at the radiofrequency signal available on the antenna cable, while provides a DC insulation of the detection section from the LNB (but guarantees the radiofrequency coupling). This voltage can be supplied by the power supply implemented inside the module, or by an external battery (to perform the measures even where the power line is not available). The choice between the battery and the power line is done automatically by the relay.

The circuit diagram of the power supply is illustrated in Figure 4. The whole supply bridge is shown in Figure 5.

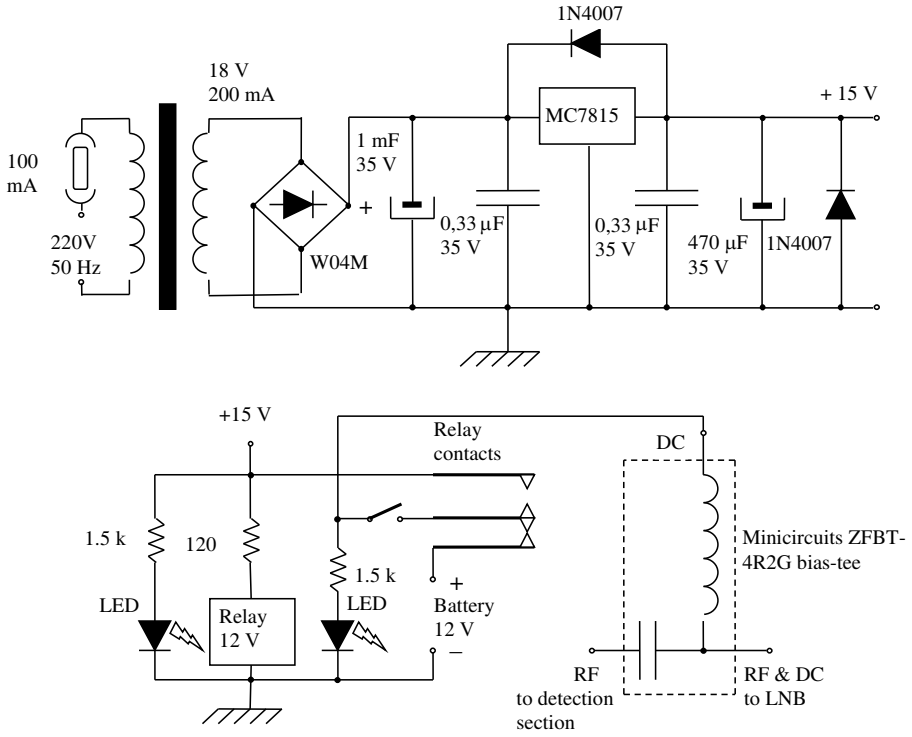

Figure 4. Circuit diagram.

4. MEASURING EQUIPMENT

The measurement system was used in several different configurations.

The first configuration uses, for the detection of the LNB output, a digital spectrum analyzer Agilent E4402B in two different settings: linear scale, Center Frequency = 1400 MHz, Span = 100 MHz, RBW = 1 MHz, VBW = 3 kHz channel power, logarithmic scale, Center Frequency = 1400 MHz, Span = 15 MHz, Integrated Band = 10 MHz, Resolution = 100 kHz, Video Resolution = 3 kHz.

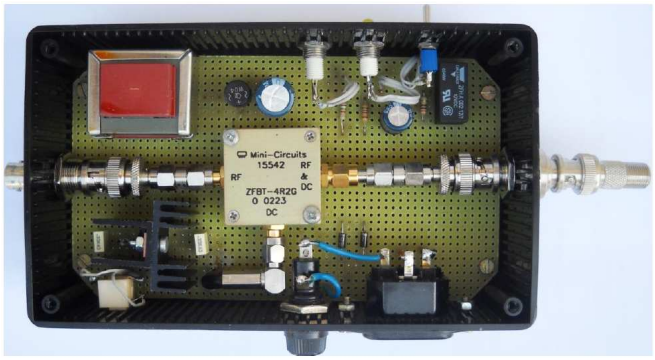

Figure 5. Supply bridge.

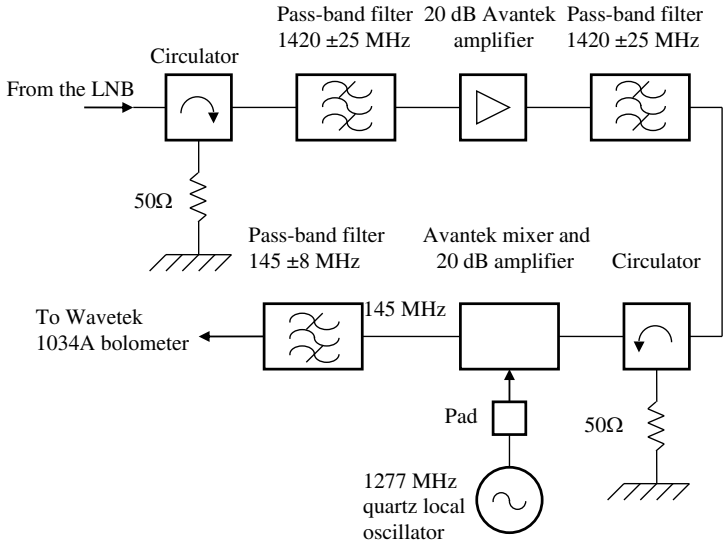

Figure 6. Block diagram of the 12 GHz receiver with band pass of 16 MHz.

The second configuration uses, as IF stage, a receiver (already available in laboratory) having a bandwidth of 16 MHz. The detector stage is a bolometer Wavetek 1034A (see Figure 6).

In the third configuration, the IF signal is amplified by a Minicircuits ZEL-0812LN (gain 20 dB) and filtered by a band pass filter 1660 ± 50 MHz. The detector stage is the bolometer (Figure 7). The fourth configuration is the same but the band pass filter is 1660 ± 100 MHz (Figure 7).

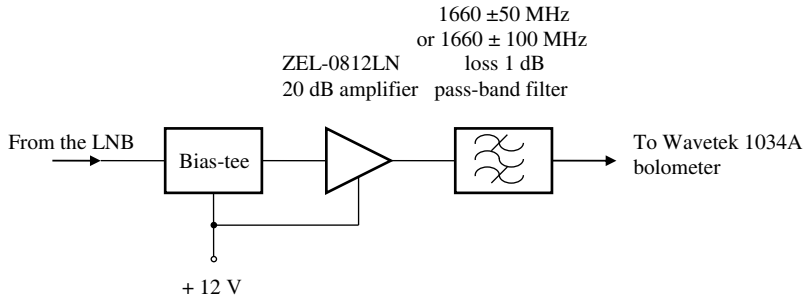

Figure 7. Block diagram of the 12 GHz receiver with band pass of 100 MHz or 200 MHz.

For the measurements of the emission of the sources indicated Table 1 and Figure 10, the LNB was mounted on the focus of a parabolic mirror. In this manner, the beam angle is reduced from 60° to

Table 1. Summary table of calculated values — measured values of the power density received from Cold Sky, Sun, Earth and an outer wall at the frequency of 12 GHz.

Source	IF band (MHz)	Calculated power density (W/m^2)	Measured power density (W/m^2)
Cold Sky	200	$0.49 \cdot 10^{-12}$	$1.11 \cdot 10^{-12}$
	100	$0.24 \cdot 10^{-12}$	$0.62 \cdot 10^{-12}$
	16	$39.43 \cdot 10^{-15}$	$116.6 \cdot 10^{-15}$
	10	$24.64 \cdot 10^{-15}$	$61.86 \cdot 10^{-15}$
	1	$2.46 \cdot 10^{-15}$	$2.17 \cdot 10^{-15}$
Sun	200	$9.60 \cdot 10^{-12}$	$5.88 \cdot 10^{-12}$
	100	$4.80 \cdot 10^{-12}$	$4.70 \cdot 10^{-12}$
	16	$768.00 \cdot 10^{-15}$	$790.68 \cdot 10^{-15}$
	10	$480.00 \cdot 10^{-15}$	$273.90 \cdot 10^{-15}$
	1	$48.00 \cdot 10^{-15}$	$41.16 \cdot 10^{-15}$
Earth	16	$244.43 \cdot 10^{-15}$	$388.63 \cdot 10^{-15}$
Sunny wall	10	$157.71 \cdot 10^{-15}$	$140.25 \cdot 10^{-15}$
	1	$15.77 \cdot 10^{-15}$	$11.96 \cdot 10^{-15}$

3°: the receiver still does not solve the source but now the "dilution effect" is acceptable. However, it should be taken into account in the measurement [9] the paraboloid efficiency, which is 60%.

5. CALIBRATION BENCH

To obtain the precise gain of the measuring system in its different configurations, a calibration bench (Figure 8) has been prepared. It consisted of:

- the measuring system, in the configurations described in paragraph 4;
- a metal surface coated with graphite varnish. The surface temperature was controlled by a probe and thermostat Eliwell IC 912 Pt100-TC that drove a heater.

The characteristics of the probe are: Measuring range: −150°C–1350°C; Precision: 0.5% + 1 digit; Resolution: 0.1°C T < 200°C, 1°C T > 200°C.

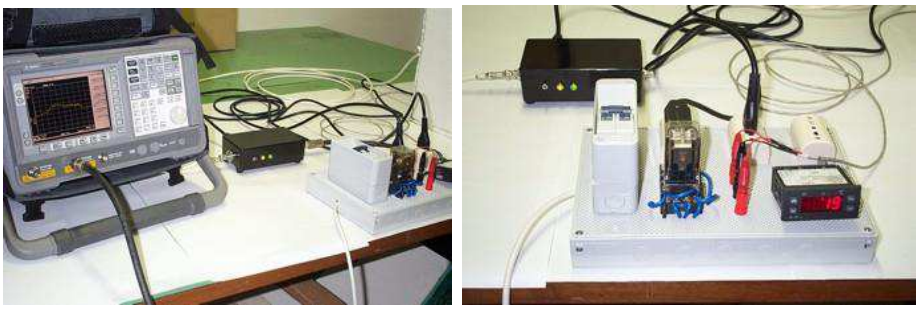

Figure 8. Spectrum analyzer, supply bridge, thermostat.

In order to avoid that the LNB measured emissions unrelated to the calibration surface, the space between the LNB and the surface was enclosed in a polystyrene box, whose inside walls were impregnated with graphite varnish (Figure 9).

The maximum measurement uncertainty that we found was approximately 10%.

We do not report the calibration table that resulted by the measurements because they depend on the LNB that it is used.

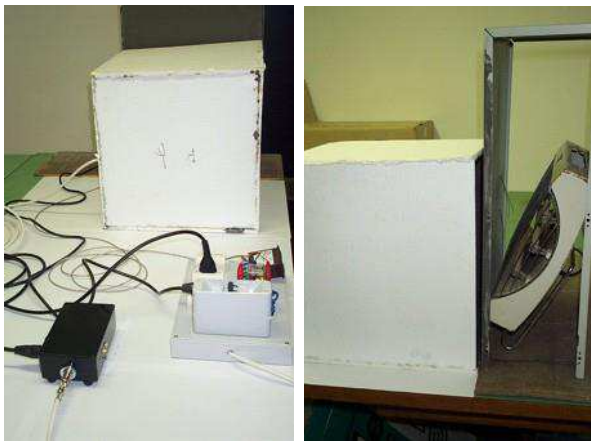

Figure 9. The LNB block is contained in the polystyrene box, whose inside walls are impregnated with graphite varnish. The emitting surface is heated by an electric heater controlled by the thermostat.

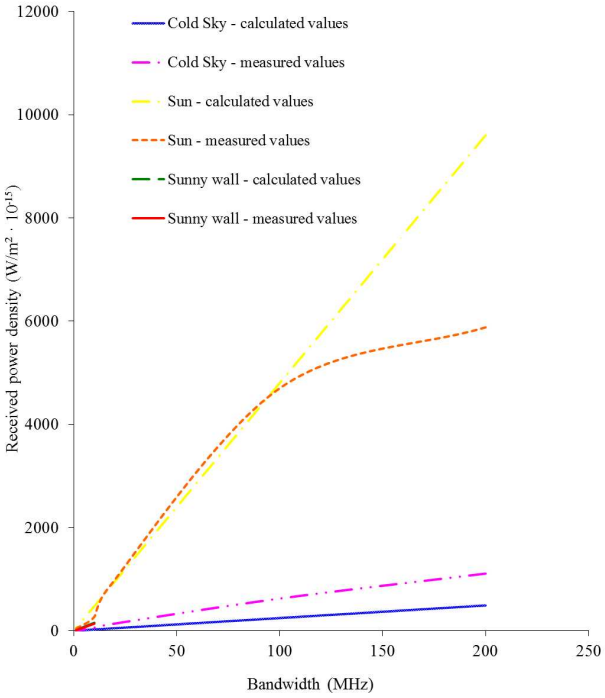

Figure 10. Graph of the received power density by the measured sources as a function of the bandwidth of the receiver. The trends of the measured and calculated values were reported.

6. MEASUREMENTS

The system, in its different configurations, was used to measure the emission due to some natural sources: Earth, Sun and a sunny wall. Table 1 summarizes the carried out measures and compare them with the calculated values [1].

From Table 1 was obtained the graph shown in Figure 10.

Well aware of the sensitivity of our system under test, a preliminary evaluation of spurious radio signals or noise sources, even those produced by any domestic appliance was systematically and

continuously performed using a spectrum analyzer connected to a small directional antenna. Beaming around sky vs horizon no trace of radio or of any other noise source were spotted to be accounted for, making trustworthy the figures quoted in the paper.

In the calculation of the measured power we took into account the sighting of the secondary lobes of the parabolic mirror: for them the manufacturer indicates an attenuation of 18 dB with respect to the main lobe.

7. DISCUSSION

For all the carried out measurements the discrepancies between the expected values and the measured values are attributable:

- to inaccurate knowledge, at the time of the measurement, of the temperature of the Earth and of the Cold Sky;
- to imperfect estimation of the noise introduced by the secondary lobes;
- to a T_R probably much greater than that calculated from the noise figure of the front-end receiver (which may be greater than that indicated by the manufacturer);
- to inaccurate knowledge of the gain of the system, because the calibration procedure does not involves all the temperatures that are subsequently measured;
- to the thermal drift of the gain of the system, in particular of the LNB;
- to possible non-linear behaviour of the amplifiers, because the power levels involved are not small.

However, we observe an acceptable match between the measured power ratios and those expected. The graph of Figure 10 shows, for the measured values, a good correspondence to the Rayleigh-Jeans law.

ACKNOWLEDGMENT

I would like to thank Dr. Goliardo Tomassetti and Prof. Gavril Grueff from I.R.A — I.N.A.F. Bologna, Professor Gabriele Falciasecca and Dott. Ana Beaven from the Università di Bologna for their kind cooperation.

REFERENCES

1. Kraus, J. D., *Radio Astronomy*, McGraw-Hill Book Company, New York, 1966.
2. Skou, N., *Microwave Radiometer Systems: Design and Analysis*, Artech House, 1989.
3. Wilson, W. J., A. B. Tanner, F. A. Pellerano, and K. A. Horgan, "Ultra stable radiometers for future sea surface salinity missions," JPL Report D-31794, 2005.
4. Camps, A. and J. M. Tarongì, "Microwave radiometer resolution optimization using variable observation time," *Remote Sensing*, Vol. 2, No. 7, 1826–1843, 2010.
5. Lionel, L. and R. Sergio, *Fisica Generale*, 2nd Edition, Milano, Casa Editrice Ambrosiana, 1983.
6. Tinti, M., "Realizzazione per mezzo di componenti a basso costo di un apparecchio dimostrativo per la misura della emissione umana di campi elettromagnetici a microonde," *Elettronica e Telecomunicazioni*, Anno LV N. 2, Centro Ricerche e Innovazione Tecnologica, RAI ISSN:0013-6123, Aug. 2006.
7. Amaduzzi, L. and M. Tinti, "Implementation of a microwave Dicke receiver," *Electronics World*, Vol. 114, No. 1864, 37, Apr. 2008.
8. Amaduzzi, L. and M. Tinti, "Low cost components radiometer implementation for human microwave electromagnetic field emission detection," *Progress In Electromagnetics Research Letters*, Vol. 23, 9–18, 2011.
9. Tinti, M., "Construction of a 12 GHz total power radio telescope for teaching purposes, suitable for noisy environments, using satellite TV devices," *Progress In Electromagnetics Research C*, Vol. 37, 159–170, 2013.